IEEE Access
Multidisciplinary | Rapid Review | Open Access Journal

Received October 29, 2016, accepted November 11, 2016, date of publication November 22, 2016,
date of current version January 4, 2017.

Digital Object Identifier 10.1109/ACCESS.2016.2631505

A Wind-Wave Farm System With Self-Energy Storage and Smoothed Power Output

XIANXIAN ZHAO, ZUANHONG YAN, AND XIAO-PING ZHANG, (Senior Member, IEEE)
School of Engineering, University of Birmingham, Birmingham, B15 2TT, U.K.

Corresponding author: X.-P. Zhang (x.p.zhang@bham.ac.uk)

This work was supported in part by the EPSRC under Grant EP/L017725/1, and Grant EP/N032888/1, in part by the University of Birmingham Siguang Li Scholarship, and in part by the China Scholarship Council.

ABSTRACT This paper proposes a wind-wave farm system with a self-energy storage capability and a smoothed total power output. The fluctuating electrical power from wave is smoothed by utilizing the rotor inertias of the wind turbines as short-term energy storage devices, thus without extra energy storage hardware the investment and maintenance cost of the wave energy conversion is reduced. This is achieved based on the fact that the wind power can be viewed as constant during a typical wave period (5∼12 s). The proposed integral compensation control of the wind turbines can optimize two conflicting objectives: maximizing wind energy capture at different wind speeds and regulating the rotor speeds of wind turbines as kinetic energy storage devices. It enables the turbine speed to swing around its optimum points at different wind speeds. Consequently, the total power output of the wind-wave farm is well smoothed at a marginal cost of the power take-off efficiency loss. RTDS simulations and quantitative analysis are presented to demonstrate the proposed system. To demonstrate its superiority, the proposed control method is compared with the direct compensation of the wave power based on the existing maximum power point tracking method.

INDEX TERMS Wind-wave farm, energy storage, power quality, maximum power point tracking (MPPT).

I. INTRODUCTION

Wave energy is gaining interests as a possible contributor to the world energy portfolio, though presently it is much less explored than the wind and solar energy. The potentially exploitable wave power resource can be of the order of 1 TW over the world [1], whilst by 2050 the global installed capacity of wave energy generation is estimated to be 46 GW [2]. Until now a number of wave energy devices have been designed. Based on the principle of energy conversion the wave energy converters (WECs) can be classified into four types: (i) oscillating water column (OWC), (ii) overtopping devices, (iii) hinged contour devices (e.g. Pelamis [3]), and (iv) point absorbers (e.g. Archimedes Wave Swing [4]).

However, the wave power generated from these devices fluctuates heavily at a typical period of 5∼12s with variation from zero to megawatts [1], [5]. When the wave power is integrated into a grid, the fluctuation raises many problems, e.g., voltage flicker, frequency variations, harmonics, and thermal excursions [6], [7]. Although the aggregation of many WECs in a wave farm has some smoothing effect, wave power smoothing is still an important and challenging issue for large-scale utilization of wave electricity production [7].

Several smoothing approaches have been developed from the WEC mechanical side by using accumulators in hydraulic devices [3], [8]. However, these approaches suffer drawbacks of high cost, low capture energy efficiency, frequent maintenance, limited installed location [9], [10], etc. Another way of wave power levelling is using short-term energy storage devices at the grid side, such as batteries [11], supercapacitors [12], [13], flywheels [14], and super conducting magnetic energy storage systems [15]. However, limitations of these solutions include the short recharge lifecycle of batteries, the large space required by the capacitors, extra cost, maintenance, and the need of extra converters and hardwares, especially in a harsh offshore environment. Therefore, a new smoothing approach with little maintenance and low cost is of our interest.

It is known that the inertia energy of wind turbine units is large and can be utilized for short-term grid frequency regulation [16], [17]. Additionally, compared with the wave power, the wind power can be viewed as constant and does not need to be smoothed at the same time scale period (5∼12s). Thus, the large inertia energy of offshore wind turbines could be used to smooth the wave power as short-term energy storage if the combined exploitation

of offshore wind and wave energies is possible and economic.

Actually, since waves are generated by wind and these two resources overlap to a large extend in nature [18], a combined harnessing of offshore wave and wind energy is now attracting great research interests and is corroborated by recent EU funded projects, such as TROPOS, ORECCA, MERMAID, MARINA and H2OCEAN [19]. The advantages of an integrated offshore wind and wave farm (wind-wave farm) include but are not limited to enhanced energy production, shared infrastructure, shared operation and maintenance, power smoothing [19]–[22]. These papers analysis and verify those benefits and show that it is a promising direction in the future to combine exploitation of wind and wave energies on a wind-wave farm. However, they do not use kinetic energy of wind turbines to smooth fluctuating wave power.

This paper proposes an Integral Compensation Control (ICC) for smoothing fluctuating wave power by using the rotor inertias of wind turbines as short-term energy storage on a basis of a wind-wave farm.

The principle of the method is to design a rotor speed controllers for wind turbines to regulate their kinetic energy as the energy storage, whist optimize the maximum wind energy capture when the wind speed changes. The wind turbine speed should be controlled at its different optimums following different wind speed to maximize the energy capture. However, it also needs to change timely as energy storage to follow the fluctuating wave power irrelevant to the wind speed. These two objectives are contradictive and to handle it a supplementary integral torque term is applied to the ICC.

The contributions of the paper are summarized as follows.

- A wind-wave farm system and its control are proposed with a smoothed power output. Compared with the existing wave power smoothing methods, the proposed ICC strategy requires no additional energy storage system.
- The ICC optimizes two conflicting objectives simultaneously, smoothing the total power output with less than 1% loss of the wind power capture efficiency.
- The wave sector of the proposed system can be any fluctuating power input. This makes the system compatible to all kinds of mainstream WECs.

The paper is organized as follows. Section II gives a system overview of the proposed wind-wave farm system and Section III presents the control methods and their developments. Simulation results in time domain and quantitative analysis of the dynamic performance and efficiency of the control methods are presented in Section IV. Finally, Section V concludes the study.

II. A WIND-WAVE FARM SYSTEM

This section presents an overview of the proposed wind-wave farm system (see Fig.1) with its wind and wave sectors. The wind sector consists of two wind turbine units represented by two DFIGs. The wave sector is presented by a general fluctuating power source with its main spectrum covering the typical range of wave periods, regardless of the prime mover

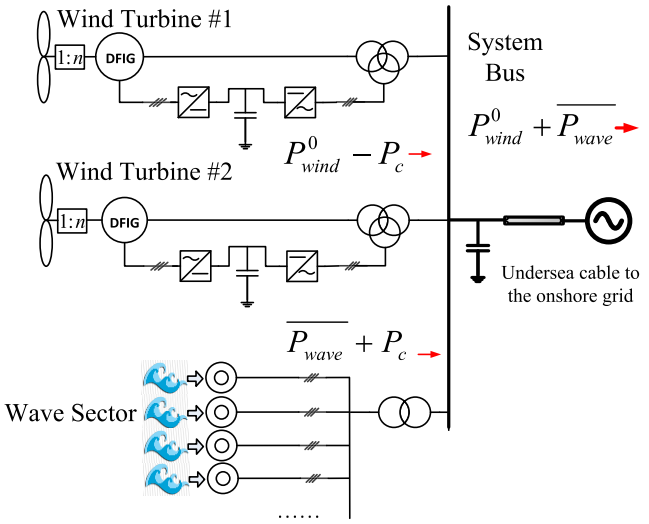

FIGURE 1. A schematic of the proposed wind-wave farm system.

interactions with the wave. This can be achieved by a group of parallel fixed speed induction generators (FSIG) with periodic driving torques of different frequencies on them.

This presentation of the wave sector is reasonable for it covers the worst case of the mainstream power take-off (PTO) designs from the grid view with its uncontrollable reactive power. Among the existing PTOs of WECs, FSIGs are exactly used in overtopping devices and Pelamis [3]. As for point absorbers, in most cases the primary electrical power is transmitted to the grid through a back-to-back converter [4], [23], whose external characteristics are equivalent to a synchronous generator with even better controllability than FSIG. As for the OWC applying DFIG, whose external characteristics to the grid are fluctuating real power and a partially controllable reactive power, which are also covered by those of the FSIGs.

A capacitor bank is connected to the system bus of the wind-wave farm (referred to as the system bus thereafter), and the farm is further connected to the onshore grid through an undersea AC cable transmission line.

In the wind-wave farm system, the wave sector without control generates fluctuating power represented by a mean $\overline{P_{wave}}$ plus a real-time varying value P_c. The electrical wind power has two parts: the wind power output P^0_{wind} from the environmental wind and the wave power compensating value $-P_c$ which is used to smooth the wave power. Compared with the wave power, P^0_{wind} can be viewed as a constant at the same time scale of the wave power period, and $-P_c$ comes from the wind turbine rotor inertias with zero-mean-value in long-term (hours). Finally the power of the system bus will be the sum of $\overline{P_{wave}}$ and P^0_{wind}, which is smooth.

III. SYSTEM CONTROL METHODS AND THEIR DERIVATIONS

For the purpose of comparison, this section begins with an introduction of the Direct Compensation of wave power

based on the existing MPPT method [24]. After that, as one of the main contributions of this paper, the proposed ICC is presented. For the sake of simplicity, the control of a single turbine is considered first, which is then extended to a multi-turbine scenario.

A. DIRECT COMPENSATION OF THE WAVE POWER

It is known that in the classical MPPT control [24], the power or toque reference of a wind turbine are given as

$$P_{ref0} = K_{opt} * w_{r1}^3 (t) \quad (1)$$

$$T_{ref0} = K_{opt} * w_{r1}^2 (t) \quad (2)$$

where $w_{r1}(t)$ is the real-time rotor speed of the turbine, $K_{opt} = 0.5\rho\pi R^5 C_{Pmax}/\lambda_{opt}^3$, C_{Pmax} is the maximum value of the coefficient of performance of the wind turbine $C_P(\lambda, \beta)$ when the pitch angle $(\beta) = 0°$, and λ_{opt} is the tip speed ratio when $C_P = C_{Pmax}$. The $C_P \sim \lambda$ curve used for this study is borrowed from [25] and [26]. The control block diagram is shown in Fig.2 (a).

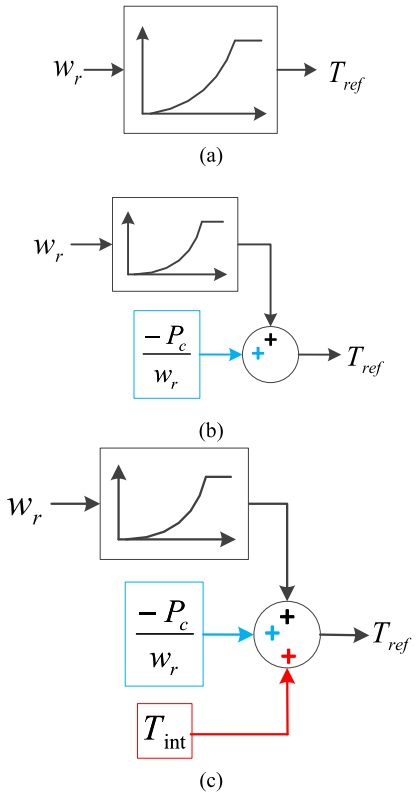

FIGURE 2. Brief control block diagrams comparison of a single turbine. (a) MPPT control. (b) Direct Compensation of wave power control. (c) Proposed Integral Compensation Control.

In the wind-wave system the Direct Compensation of the wave power control has two objectives:

- *Maximum power capture*. Ensure the DFIG can follow the change of the wind speed and work at its optimum rotor speed.
- *Smoothing wave power*. Using stored kinetic energy of the rotor to deliver a real-time power fluctuating oppositely to that of the wave energy sector.

Define the wave power to be smoothed as

$$P_c = P_{wave} - \overline{P_{wave}} \quad (3)$$

where P_{wave} and $\overline{P_{wave}}$ are the real-time output power and average output power of the wave sector, respectively. $\overline{P_{wave}}$ is given by the Moving Average Filter, which averages the real-time wave power in a moving window period of time.

To smooth the fluctuating power P_c, an immediate idea is to introduce an additional term $-P_c$ to (1) to generate an opposite compensation of it. In this way, (1) becomes

$$\begin{aligned} P'_{ref} &= P_{ref0} - P_c \\ &= K_{opt} * w_{r1}^3 (t) - P_c \end{aligned} \quad (4)$$

and the torque reference (Fig. 2 (b)) is

$$T'_{ref} = K_{opt} * w_{r1}^2(t) - P_c / w_{r1}(t). \quad (5)$$

Therefore, at a constant wind speed (with a related optimum rotor speed w_{r_opt}), we expect to have an ideal form of DFIG torque

$$T''_{ref} = K_{opt} * w_{r_{opt}}^2 - P_c / w_{r1}(t) \quad (6)$$

to achieve the objectives of maximum power point tracking and wave power smoothing.

The Direct Compensation method as shown in Fig. 2(b) uses the control reference from (5) to achieve the control objectives. It should be mentioned that the desired control reference in (6) cannot be fully realized by the input toque reference (5). This is due to the fact that the additional $-P_c$ accelerates the turbine and thus the real-time rotor speed $w_{r1}(t)$ moves away from the optimum value w_{r_opt}. Although the term $-P_c/w_{r1}(t)$ in (5) can smooth the fluctuating wave power, the term $K_{opt} * w_{r1}^2(t)$ introduces new fluctuation to the output power injected to the system bus. This problem prevents the Direct Compensation design (5) from achieving the prescribed control objectives and hence this needs to be solved. To this end, a more rigorous control method will be derived – the proposed ICC in the next section.

B. THE PROPOSED INTEGRAL COMPENSATION CONTROL

To solve the aforementioned problem one might think of using (6) as the torque reference directly. This method can smooth the wave power and approximately realize the maximum power point tracking at a constant wind speed. However, the turbine is unstable when the wind speed changes, since $K_{opt} * w_{r\_opt}^2$ contains no feedback of the real-time rotor speed.

Another alternative is to achieve an equivalent (6) with a feedback of $w_{r1}(t)$. So we go back to use (5) yet with an additional term T_{int} as

$$T_{ref} = K_{opt} * w_{r1}^2(t) - P_c / w_{r1}(t) + T_{int}. \quad (7)$$

To equalize (6) and (7), it has

$$T_{int} = -K_{opt} * \left(w_{r1}^2(t) - w_{r\_opt}^2 \right). \quad (8)$$

During the acceleration of the rotor from a speed of w_{r_opt} to $w_{r1}(t)$, the variation of the kinetic energy ΔE stored in the rotor is

$$\Delta E = \int (P_c + \Delta P)dt \tag{9}$$

where ΔP is the difference between the maximum power which the wind turbine can capture at the wind speed and the instantaneous captured power due to the change of the wind turbine rotor speed, as is shown in Fig. 3. It is also noted that

$$\Delta E = \frac{1}{2} \cdot J \left(w_{r1}^2(t) - w_{r_{opt}}^2 \right) \tag{10}$$

where J is the total inertia of the turbine rotor.

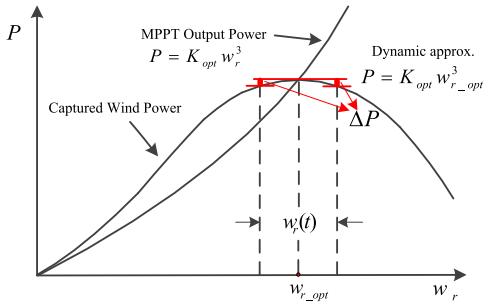

FIGURE 3. The power-speed characteristic of a wind turbine swinging around an optimum point at a wind speed.

From (9) and (10), we have

$$w_{r1}^2(t) - w_{r_{opt}}^2 = \frac{2}{J} \int (P_c + \Delta P)dt. \tag{11}$$

From (9) and (11),

$$T_{int} = \frac{-2 \cdot K_{opt}}{J} \int (P_c + \Delta P)dt. \tag{12}$$

Now we need to make an assumption that ΔP is sufficiently small and can be ignored. This is validated by the simulation results of the small speed bias in Section IV. This assumption is needed because in engineering practice, the mechanical power from the captured wind is difficult to measure. Even if an accurate expression including the effect of ΔP can be achieved, the improvement of the power capture efficiency and power smoothing performance is limited. With this assumption, we have

$$T_{int} = \frac{-2 \cdot K_{opt}}{J} \int P_c dt. \tag{13}$$

Finally, from (7) and (13) the ICC control torque reference of a single turbine (Fig. 2 (c)) is

$$T_{ref} = K_{opt} \cdot w_{r1}^2(t) + \frac{-P_c}{w_{r1}(t)} + \frac{2 \cdot K_{opt}}{J} \int (-P_c)dt. \tag{14}$$

From (14), the control power reference is

$$\begin{aligned} P_{ref} &= K_{opt} \cdot w_{r1}^3(t) + w_{r1}(t) \cdot \frac{2K_{opt}}{J} \int (-P_c)dt - P_c \\ &= P_{wind}^0 - P_c \end{aligned} \tag{15}$$

where $P_{wind}^0 = K_{opt} \cdot w_{r1}^3(t) + w_{r1}(t) \cdot \frac{2K_{opt}}{J} \int (-P_c)dt$. Note that this work uses the torque as the input reference of the DFIG, but the power reference can also be used.

Summarizing, the single turbine control system with the proposed ICC is given in Fig. 4, which ensures the turbine rotors swinging around its optimum speed according to the real-time wind speed when it plays the role of energy storage at the same time.

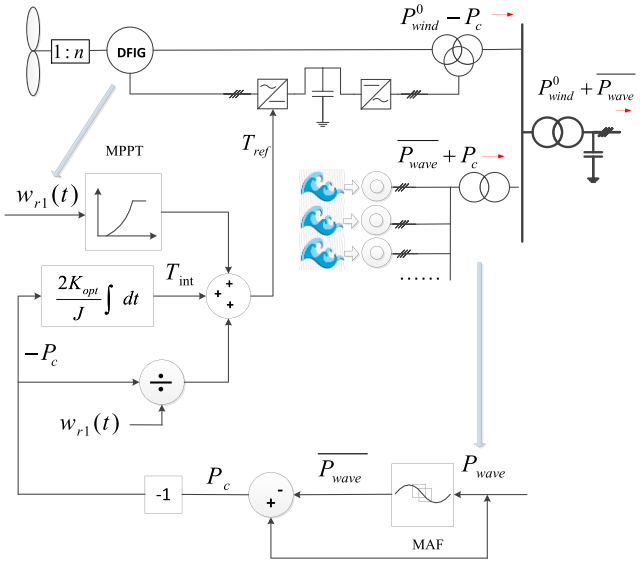

FIGURE 4. The ICC of a single turbine in the wind-wave farm system.

The proposed ICC only requires the measurements of the rotor speed of the turbine and the electric power from the wave energy sector, both of which are conveniently accessible.

C. COORDINATION OF MULTIPLE TURBINES

In a wind-wave farm system with multiple wind turbines, the control of the torque reference of each turbine is the same as above, except that $-P_c$ is replaced by $-P_{ci}$ because the i^{th} turbine only needs to respond to part of the total compensation wave power required, i.e. $-P_c$. Since the kinetic energy stored in the rotor is proportional to the square of the speed, $-P_{ci}$ is set as

$$-P_{ci} = \frac{\bar{w}_{ri}^2(t)}{\sum_{j=1}^{M} \bar{w}_{rj}^2(t)} \cdot (-P_c) \tag{16}$$

where $\bar{w}_{ri}(t)$ is the average value of the rotor speed by a moving average filter. Then we always have

$$\sum_{i=1}^{M} (-P_{ci}) = -P_c \tag{17}$$

where M is the total number of wind turbines.

Another reason of allocating the compensating power according to the rotor speed is that such an application helps to reduce the total loss of the wind power capture efficiency. When the speed bias is evenly distributed among turbines,

the rotor with a higher speed would naturally release more energy.

IV. SIMULATION RESULTS

Two prototypes of the proposed wind-wave farm were built and case studies were carried out on RTDS under different conditions. One test system consists of one wind turbine and three wave generators (referred to as "one-turbine system") to study the control of a single turbine and another test system is composed of two wind turbines and six wave generators (referred to as "two-turbine system") to study the coordination of multiple turbines. The simulation parameters are listed in Table I in the appendix. The rotating mass of the turbine is presented by a two-mass shaft model. The driving torques on the wave generators are simulated by a group of sinusoidal waves with random frequencies, phases, and magnitudes to model a real sea wave condition. The time period of waves are selected within a typical range of $5 \sim 12$s.

Simulations are performed using the following 5 cases, among which Cases 1∼4 are using the one-turbine system while Case 5 is using the two-turbine system.

Case 1: Time series simulations under a constant wind speed by using the ICC.

Case 2: Dynamic performance with the proposed ICC method.

Case 3: Comparison of the system performance of the Direct Compensation with that of the ICC.

Case 4: Dynamic performance under variable wind speed.

Case 5: Demonstration of the coordination of multiple turbines on a two-turbine system.

A. CASE 1

This case studied the performances of the proposed ICC with the one-turbine system under a constant wind speed ($V_w = 9.5\ m/s$).

Figure 5 shows that the injected power of the wind-wave farm to the system bus is well smoothed after the proposed ICC is activated at $t = 120$s. Meanwhile, the rotor speed of the DFIG is swinging slightly around the optimum rotor speed accordingly when the rotor inertia of the turbine works as flywheel energy storage, while the DFIG releases instantly big power output and generates the related fluctuating output power. From the third diagram, it can be seen that the average of the wind output power of the blue line is almost equal to the red dash line. This illustrates that the loss of the wind power is very small when it comes to smooth the wave power.

Based on that the wind power loss is caused mainly by the speed bias, and it is expected that bigger rotor inertia of a wind turbine, bigger wind speed input or less fluctuating wave power to be smoothed could reduce the speed bias and consequently reduce the power loss.

B. CASE 2

This case presents a quantitative analysis of the smoothing effect and the wind-capture efficiency of the wind-wave farm system when the wind-wave ratio ξ changes. The wind-wave

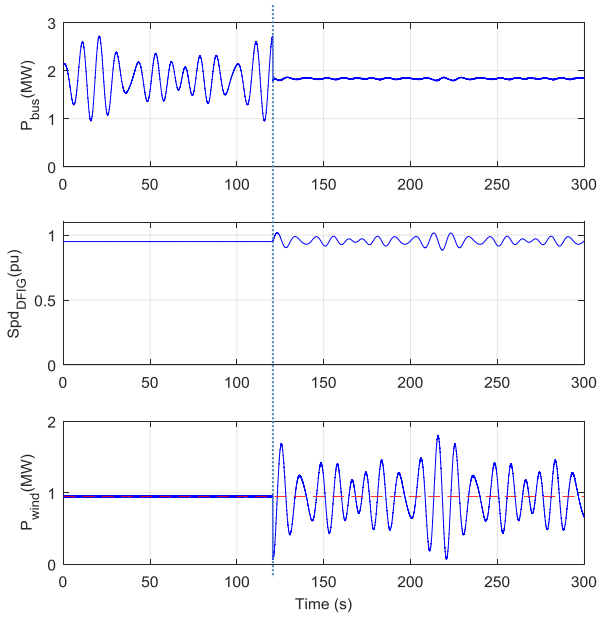

FIGURE 5. The total power injected to the system bus (Bus Power), the DFIG rotor speed, and the DFIG output power before and after the proposed ICC activated (the dotted vertical line). The red dash represents the output power under the MPPT control.

ratio ξ is a pure number without unit, which is defined as

$$\xi = \overline{P_{wind}}/\sigma_{wave} \tag{18}$$

where $\overline{P_{wind}}$ is the average electrical output power from the wind sector when it does not smooth the total power output, and σ_{wave} is the standard deviation of the electrical power from the wave sector. This index assesses the necessary scale of the wind sector to achieve the smoothing effect of the whole wind-wave farm system with a given degree of the wave power fluctuation.

Two quantitative indexes of the wind-wave farm system are of our particular interests. One is the standard deviation of the total output power to the system bus σ_{bus}, which represents the smoothing effect. Another is the wind power capture efficiency η, which is defined as the ratio of the average electrical power from the wind sector under the classical MPPT control over that under the proposed ICC with all other conditions the same. $(1-\eta)$ represents the lost percentage of the captured wind power from its optimum as a cost of the power smoothing effect.

Figure 6 shows these two indexes of the simulated system under different ξ. As can be seen, with the power smoothing control, σ_{bus} is significantly reduced by 10-20 times at a cost of about 1% loss of the wind power capture efficiency under ξ bigger than 2. The results also show that a bigger ξ helps reducing the power loss, which is smaller than 0.5% when ξ is over 2.6. This means that with less than 0.5% energy capture loss, a wind turbine which has 2.6 MW average wind output power under MPPT control can smooth the wave power with a standard deviation of 1 MW.

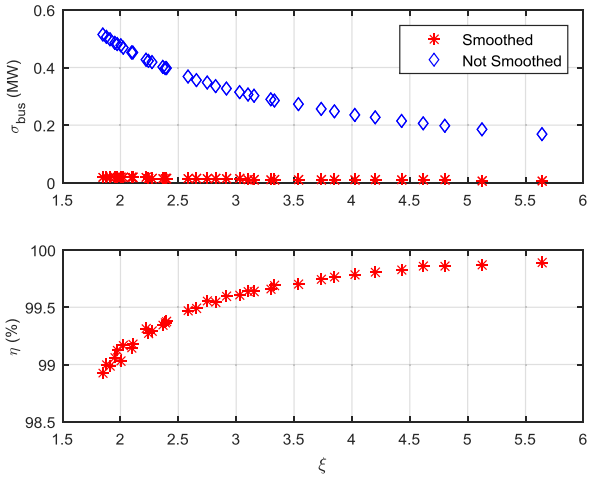

FIGURE 6. The standard deviation of the total power injected to the system bus (σ_{bus}), and the wind power capture efficiency (η) under different ratio ξ.

C. CASE 3

This case compared the performances of the Direct Compensation and the ICC on the one-turbine system at $V_w = 12m/s$.

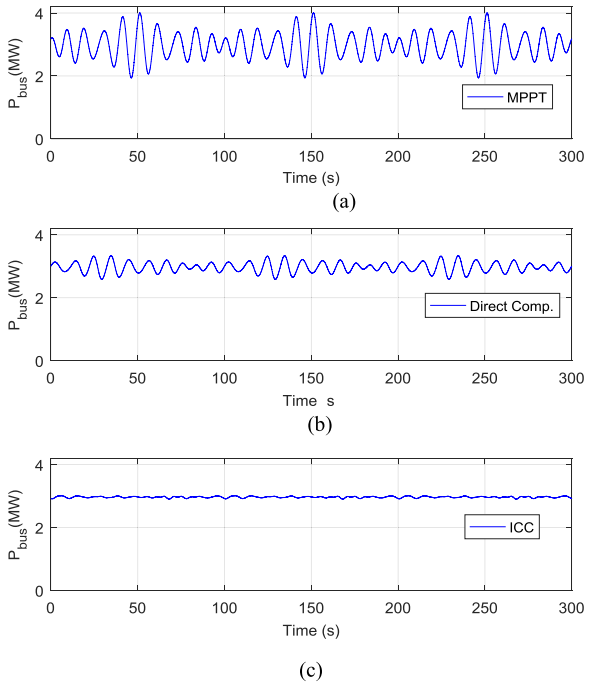

FIGURE 7. The total power injected to the system bus (Bus Power). (a) The classical MPPT control. (b) The Direct Compensation control. (c) The Integral Compensation Control.

Figure 7 shows that the Direct Compensation control has limited smoothing effect, while by introducing the integral torque term, the ICC can smooth the total power of the system bus well.

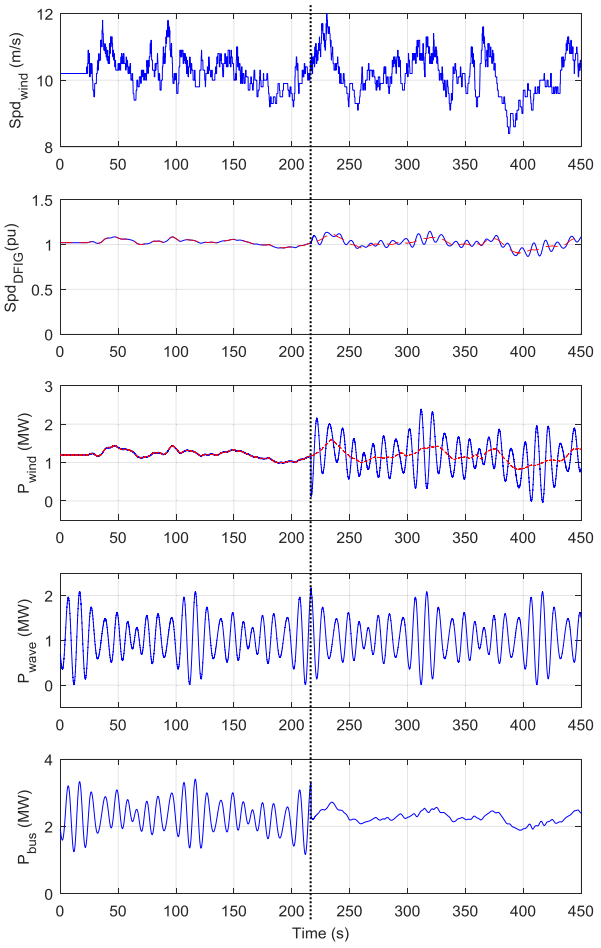

FIGURE 8. Wind speed, rotor speed, wind output power, wave output power and total power injected to the system bus (Bus Power) before and after the proposed ICC is activated (the dotted vertical line). The red dash lines represent the related quantities under the classical MPPT control.

D. CASE 4

In Case 4, the single turbine system was operated at a variable wind speed. The real-time wind data can be found in [27]. The simulation results of Case 4 are shown in Fig. 8. The ICC was activated at $t = 218$s. The red dash lines show the related quantities under the classical MPPT control with the same wind speeds input.

It can be seen from the third diagram that the wind output power under the MPPT control (represented by the red dash line) is rather smoothed. This illustrates that the wind power does not need to be smoothed during a typical wave period (5∼12s). Then the fluctuating power of the system bus comes almost from the wave power.

After the ICC is activated, it can be seen that the rotor speed of the turbine swings always around its optimum (around the red dash line in the second diagram) when the wind speed changes. This illustrates that the ICC can make the wind turbine to maximize energy capture and behave as flywheel energy storage. The maximization of wind energy capture can also be seen from the third diagram where the wind output

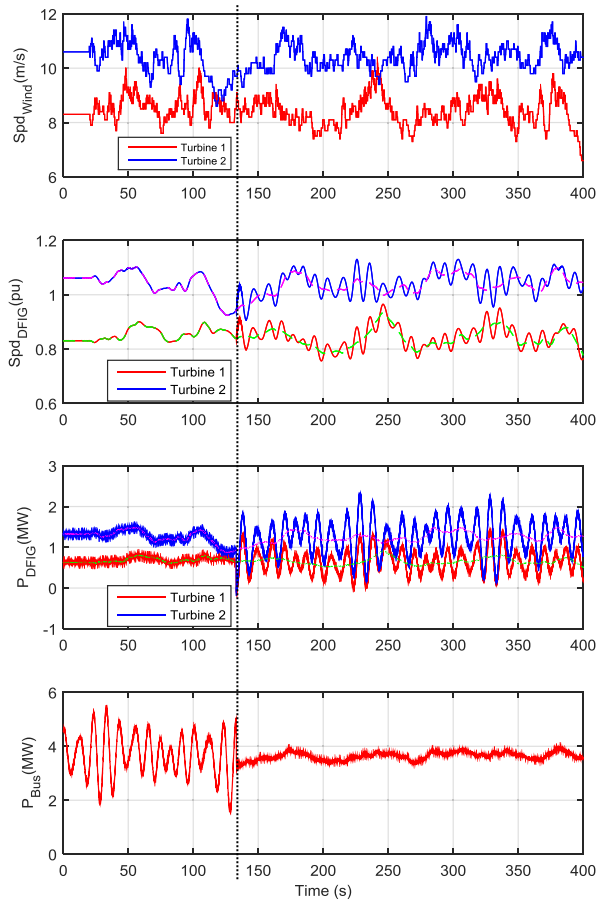

FIGURE 9. Wind speed, rotor speed, output power of each turbine, and the total power injected to the system bus (Bus Power) in a two-turbine system before and after the proposed ICC activated (the dotted vertical line). The dash lines represent the related quantities under the classical MPPT control.

power is always around the red dash line. In this case, the wind power capture efficiency η (which is calculated by the ratio of the average of the blue and red line in the third diagram during the time of 218-450s) is 99.56857% with the $\xi = 2.60115$ (average of the blue line in the third diagram divides the standard deviation of the blue line in the fourth diagram during the time of 218-450s). This data of $\xi \sim \eta$ accords with that in Fig.6.

Finally with the ICC the power of the system bus is well smoothed and tracks the long-term average of the total captured wind and wave power very well.

E. CASE 5

This case verifies that the coordination algorithm proposed in (16) can automatically allocate the compensating power among wind turbines in a multi-turbine system. The two-turbine system was studied in this case, and different wind speed time series simulations were applied on the two turbines.

From Fig. 9, the total power injected to the system bus is smoothed as that in the other cases. The compensating power, as the fluctuating part of the DFIG output power, is allocated among all the participating turbines according to their average rotor speeds. As can be seen, a wind turbine with a higher wind speed which has bigger rotor speed and higher level of wind output power is related to a larger fluctuation, which is exactly suggested by (16).

At the same time, it can be seen that the fluctuation of the speed of each turbine are almost in the same range. This minimizes the total loss of the wind power capture efficiency as the speed bias is evenly distributed. Additionally, the figures in further verify that the rotor speeds can always swing around their optimums following the change of the wind speeds as illustrated above.

TABLE 1. Simulation parameters.

Symbol	Quantity	Value
DFIGs		
Sb	rated power	2.2 MVA
Vb	rated line-line rms voltage	0.69 V
fb	rated frequency	50 Hz
Rs	rotor resistance	0.00462p.u.
Rr	rotor resistance	0.0060p.u.
Ls	stator leakage inductance	0.102p.u.
Lr	rotor leakage inductance	0.08596p.u.
Lm	mutual inductance	4.348p.u.
k	rotor over stator turns ratio	2.6377
Ht	wind turbine inertia constant	4.3s
Hg	DFIG inertia constant	0.75s
Cd	dc link capacitance	10 e3μF
Li	GSC side inductance	120 e-6 H
Ri	GSC side resistance	0.0015 Ω
kdfig	three winding transformer turn ratio	22/0.69/0.69
Wave sector FSIGs		
Sb	rated power	0.4 MVA
Vb	rated line-line rms voltage	0.825 kV
fb	rated frequency	50 Hz
Rs	stator resistance	0.00365 p.u.
Rr	rotor resistance	0.0039 p.u.
Ls	stator leakage inductance	0.06 p.u.
Lr	rotor leakage inductance	0.1203 p.u.
Lm	mutual inductance	3.0 p.u.
H	inertia constant	3.053s
kwave	wave transformer turn ratio	22/0.825
Tw	period of the wave power	5~12s
The onshore grid		
Vinf	infinite grid line-to-line rms voltage	22kV
SCR	local short-circuit ratio	10

V. CONCLUSION

This paper has proposed a wind-wave farm system with a self-energy storage capability. Based on the fact that the electrical power from the wind sector can be viewed as constant during a typical wave period, the proposed system uses the rotor inertias of the wind turbines as the short-term energy storage to smooth the fluctuating power from the wave sector. This design stands on the trend of combining the wind and wave power production together, and enjoys the advantage of delivering smoothed power output to the local grid without additional energy storage devices.

Conventionally, a key challenge to this attempt is that the variation of the kinetic energy stored in the rotor of a wind turbine leads to a bias of the rotor speed from its optimum and reduces the wind power capture efficiency. In this paper, this contradiction is alleviated by the proposed ICC, which smooths the total power output of the wind-wave farm at a marginal cost of the loss of the wind power capture efficiency. In a multi-turbine system, the proposed coordination algorithm dynamically allocates the compensating power among all the participating turbines. The proposed wind-wave farm system is compatible with both the DFIG and full rated converter based wind generators and all the four mainstream WEC devices.

The paper defines the wind-wave ratio ξ of a wind-wave farm, and presents a quantitative analysis of the system based on this index. Two prototypes of the proposed system were simulated using RTDS on five different cases. The proposed control method ICC has been compared with the classical MPPT method in terms of the wind-capture efficiency and the output power quality they can deliver. The results have demonstrated the self-energy storage and power smoothing capability of the system. It has been shown that the ICC can reduce the standard deviation of the total output power by 10-20 times with a loss of the wind-capture efficiency less than 1%. Moreover, a bigger wind-wave ratio ξ helps reducing the efficiency loss. System operations based on real wind speed profiles and the coordination of multiple wind turbines have also been presented.

APPENDIX

See Table 1.

REFERENCES

[1] H. Polinder and M. Scuotto, "Wave energy converters and their impact on power systems," in *Proc. Int. Conf. Future Power Syst. (FPS)*, 2005, pp. 1–9.

[2] X. P. Zhang and P. Zeng, "Marine energy technology," *Proc. IEEE*, vol. 101, no. 4, pp. 862–865, Apr. 2013.

[3] R. Henderson, "Design, simulation, and testing of a novel hydraulic power take-off system for the Pelamis wave energy converter," *Renew. Energy*, vol. 31, no. 2, pp. 271–283, 2006.

[4] F. Wu, X. P. Zhang, P. Ju, and M. J. H. Sterling, "Modeling and control of AWS-based wave energy conversion system integrated into power grid," *IEEE Trans. Power Syst.*, vol. 23, no. 3, pp. 1196–1204, Aug. 2008.

[5] F. O. de Antonio, "Wave energy utilization: A review of the technologies," *Renew. Sustain. Energy Rev.*, vol. 14, no. 3, pp. 899–918, 2010.

[6] A. Blavette, D. L. O'Sullivan, R. Alcorn, T. W. Lewis, and M. G. Egan, "Impact of a medium-size wave farm on grids of different strength levels," *IEEE Trans. Power Syst.*, vol. 29, no. 2, pp. 917–923, Mar. 2014.

[7] S. Armstrong, E. C. Sanchez, and T. Kovaltchouk, "Assessing the impact of the grid-connected pacific marine energy center wave farm," *IEEE Trans. Emerg. Sel. Topics Power Electron.*, vol. 3, no. 4, pp. 1011–1020, May 2015.

[8] M. F. Hsieh, I. H. Lin, D. G. Dorrell, M. J. Hsieh, and C. C. Lin, "Development of a wave energy converter using a two chamber oscillating water column," *IEEE Trans. Sustain. Energy*, vol. 3, no. 3, pp. 482–497, Jul. 2012.

[9] J. K. H. Shek, D. E. Macpherson, M. A. Mueller, and J. Xiang, "Reaction force control of a linear electrical generator for direct drive wave energy conversion," *IET Renew. Power Generat.*, vol. 1, no. 1, pp. 17–24, Mar. 2007.

[10] N. Hodgins, O. Keysan, A. S. McDonald, and M. A. Mueller, "Design and testing of a linear generator for wave-energy applications," *IEEE Trans. Ind. Electron.*, vol. 59, no. 5, pp. 2094–2103, May 2012.

[11] F. Wu, X. P. Zhang, and P. Ju, "Application of the battery energy storage in wave energy conversion system," in *Proc. Int. Conf. Sustain. Power Generat. Supply (SUPERGEN)*, 2009, pp. 1–4.

[12] D. B. Murray, J. G. Hayes, D. L. O'Sullivan, and M. G. Egan, "Supercapacitor testing for power smoothing in a variable speed offshore wave energy converter," *IEEE J. Ocean. Eng.*, vol. 37, no. 2, pp. 301–308, Apr. 2012.

[13] T. Kovaltchouk, B. Multon, H. B. Ahmed, J. Aubry, and P. Venet, "Enhanced aging model for supercapacitors taking into account power cycling: Application to the sizing of an energy storage system in a direct wave energy converter," *IEEE Trans. Ind. Appl.*, vol. 51, no. 3, pp. 2405–2414, May 2015.

[14] T. Yoshida, M. Sanada, S. Morimoto, and Y. Inoue, "Study of flywheel energy storage system for power leveling of wave power generation system," in *Proc. 15th Int. Conf. Elect. Mach. Syst. (ICEMS)*, Oct. 2012, pp. 1–5.

[15] Z. Nie, X. Xiao, Q. Kang, R. Aggarwal, H. Zhang, and W. Yuan, "SMES-battery energy storage system for conditioning outputs from direct drive linear wave energy converters," *IEEE Trans. Appl. Supercond.*, vol. 23, no. 3, p. 5000705, Jun. 2013.

[16] J. M. Mauricio, A. Marano, A. Gómez-Expósito, and J. L. M. Ramos, "Frequency regulation contribution through variable-speed wind energy conversion systems," *IEEE Trans. Power Syst.*, vol. 24, no. 1, pp. 173–180, Feb. 2009.

[17] S. Ghosh, S. Kamalasadan, N. Senroy, and J. Enslin, "Doubly fed induction generator (DFIG)-based wind farm control framework for primary frequency and inertial response application," *IEEE Trans. Power Syst.*, vol. 31, no. 3, pp. 1861–1871, May 2016.

[18] J. Brooke, *Wave Energy Conversion*, vol. 6. Amsterdam, The Netherlands: Elsevier, 2003.

[19] C. P. Collazo, D. Greaves, and G. Iglesias, "A review of combined wave and offshore wind energy," *Renew. Sustain. Energy Rev.*, vol. 42, pp. 141–153, Feb. 2015.

[20] E. Tedeschi, E. Robles, M. Santos, O. Duperray, and F. Salcedo, "Effect of energy storage on a combined wind and wave energy farm," in *Proc. IEEE Energy Convers. Congr. Exhibit., (ECCE)*, Sep. 2012, pp. 2798–2804.

[21] E. D. Stoutenburg and M. Z. Jacobson, "Reducing offshore transmission requirements by combining offshore wind and wave farms," *IEEE J. Ocean. Eng.*, vol. 36, no. 4, pp. 552–561, Oct. 2011.

[22] S. Astariz and G. Iglesias, "Output power smoothing and reduced downtime period by combined wind and wave energy farms," *Energy*, vol. 97, pp. 69–81, Feb. 2016.

[23] M. G. S. Prado, F. Gardner, M. Damen, and H. Polinder, "Modelling and test results of the archimedes wave swing," *Proc. Inst. Mech. Eng. A, J. Power Energy*, vol. 220, no. 8, pp. 855–868, 2006.

[24] R. Pena, J. C. Clare, and G. M. Asher, "Doubly fed induction generator using back-to-back PWM converters and its application to variable-speed wind-energy generation," *IEE Proc.-Elect. Power Appl.*, vol. 143, no. 3, pp. 231–241, May 1996.

[25] J. G. Slootweg, S. W. H. D. Haan, H. Polinder, and W. L. Kling, "General model for representing variable speed wind turbines in power system dynamics simulations," *IEEE Trans. Power Syst.*, vol. 18, no. 1, pp. 144–151, Feb. 2003.

[26] *Wind Turbine*, Documentation SimPowerSystems, Mathworks, Natick, MA, USA, 2004.

[27] *An Aeroelastic Computer-Aided Engineering Tool for Horizontal Axis Wind Turbines*, last modified on Mar. 19, 2015. [Online]. Available: https://nwtc.nrel.gov/FAST

XIANXIAN ZHAO was born in Hunan, China, in 1989. She received the B.Eng. degree from South China University, Hunan, in 2012. She is currently pursuing the Ph.D. degree with the University of Birmingham. Her research interests include renewable energy conversion control and applications and energy storage systems.

ZUANHONG YAN was born in Nanjing, China, in 1990. He received the B.Eng. degree from the Huazhong University of Science and Technology, Wuhan, China, and the University of Birmingham, Birmingham, U.K., in 2012, and the M.Sc. degree from The University of Manchester, Manchester, U.K., in 2013. He is currently pursuing the Ph.D. degree with the University of Birmingham. His research interests include renewable energy conversion and integration, wave farm system, and energy storage system.

XIAO-PING ZHANG (M'95–SM'06) He received the B.Eng., M.Sc., and Ph.D. degrees from Southeast University, China, in 1988, 1990, and 1993, respectively, all in electrical engineering. He was an Associate Professor with The University of Warwick, England, U.K. He was with the China State Grid EPRI (NARI Group) on EMS/DMS advanced application software research and development from 1993 to 1998. From 1998 to 1999, he was visiting UMIST. From 1999 to 2000, he was an Alexander-von-Humboldt Research Fellow with the University of Dortmund, Germany. He is currently a Professor of Electrical Power Systems with the University of Birmingham, U.K. He is also the Director of Smart Grid, Birmingham Energy Institute and the Co-Director of the Birmingham Energy Storage Center. He has co-authored the first and second edition of the monograph *Flexible AC Transmission Systems: Modeling and Control*, published by Springer in 2006, and 2012, respectively. He has co-authored the book *Restructured Electric Power Systems: Analysis of Electricity Markets with Equilibrium Models*, published by the IEEE Press/Wiley in 2010. He pioneered the concept of Global Power & Energy Internet, Energy Union, and UK's Energy Valley.